Consequences of Ca codoping in YAlO$_3$:Ce single crystals

Federico Moretti*[a]†, Karine Hovhannesyan[b], Marina Derdzyan[b], Gregory A. Bizarri[c], Edith D. Bourret[c], Ashot Petrosyan[b], and Christophe Dujardin*[a]

Abstract: The influence of Ca codoping on the optical absorption, photo-, radio-, and thermo-luminescence properties of YAlO$_3$:Ce (YAP:Ce) crystals has been studied for four different calcium concentrations from 0 to 500 ppm. Ca cooping results in partial oxidation of Ce^{3+} into Ce^{4+}. The luminescence time response under pulsed X-ray excitation of the Ce^{3+}/Ce^{4+} admixture clearly demonstrates the role of hole migration on both the rise time and the generally observed slow components. From an application point of view, Ca-codoping significantly improves the timing performances but the induced presence of Ce^{4+} ions is also the cause of a reduction in scintillation efficiency.

Introduction

Scintillators are a class of materials which are able to efficiently emit a bunch of photons in the ultraviolet-visible region of the electromagnetic spectrum following the interaction with a ionizing particle. They are thus currently used for radiation detection in several applicative sectors which span from medical and industrial X-ray and nuclear imaging, nuclear safety and security to high energy physics calorimetry.[1-4] Considering their wide possible use, it does not come as a surprise that they are currently the subject of intense research and development efforts.[5]

Light emission from a scintillator is only the last of a complex sequence of processes which start with the initial interaction of the ionizing particle with the material resulting in the creation of a large number of lower energy free electrons and holes; these are later thermalized and transferred to the luminescence centres, where they finally recombine giving rise to the UV-Vis light emission. During the thermalization and transfer stages, in particular, free electron and holes diffuse through the material covering distances of the order of few tens to few hundreds of nanometres.[6,7] These large diffusion distances make the thermalization and transfer processes particularly sensitive to the presence of carriers trapping phenomena. Beside carrier self-trapping,[8] point defects - intrinsic and extrinsic - can act as traps for free carriers slowing down, while not stopping altogether, their migration toward the recombination centres. The competition

ultimately responsible for the degradation of the scintillator performances with a reduction of light yield, the presence of rise time and long scintillation time decays, even sometimes afterglow, and luminescence sensitisation (also called bright burn or hysteresis).[9,10]

The defect impact on the scintillation process is well known, and several synthesis strategies (from aliovalent codoping to solid solution and band gap engineering)[11-15] have been proposed to reduce the concentration of traps or their relevance upon the scintillation economy. In particular, codoping with alkaline earth ions of Ce doped garnets and silicates has proven itself as a very effective way to improve these matrices scintillation timing and light yield performances with a substantial reduction of the long lived scintillation decay tails.[16-19] The detected improvements are related to the partial oxidation, induced by the codopant presence, of cerium ions into their tetravalent form. Although Ce^{4+} is not photoluminescent by itself, it can still take part in the scintillation process: Ce^{4+} ions are indeed supposed to easily and quickly capture electrons, becoming temporarily trivalent and able to give rise to the typical Ce^{3+} luminescence.[16,20,21] The introduction of this new recombination channel strongly reduces the probability for electrons to be temporarily, or permanently, trapped on defect sites thus reducing the amount of delayed recombination processes.

In this contribution, we apply the codoping strategy to clearly establish the role of hole migration and capture on the timing performances, and to evaluate the applicability of Ca-codoping to improve the scintillation characteristic of a well-known scintillator: YAlO$_3$:Ce (YAP:Ce). Four different Ca concentrations combined with two cerium concentration differing by 1 order of magnitude in YAP:Ce single crystals grown by the Czochralski method are considered. Optical absorption, steady state and sub-nanosecond time resolved radio- and photo-luminescence, as well as thermoluminescence results are used to determine the impact of Ca codoping on the optical properties of this material.

Results and Discussion

Optical absorption (OA) measurements obtained on all 2 mm thick YAP:Ce,Ca samples (fig. 1-A) substantiate very strong absorptions for wavelength shorter than 400 nm which cannot be fully followed because of absorption saturation. In the case of the sample doped exclusively with Ce, these absorptions are related to Ce^{3+} 4f-5d dipole allowed transitions.[22,23] As the Ca concentration is increased, the absorption threshold (see inset i of figure 1-A, where the wavelength at which the absorption coefficient reaches 25 cm^{-1} is reported) is shifted toward longer

[a] Dr. F. Moretti, Prof. C. Dujardin
Institut Lumière Matière, UMR55306 Université Claude Bernard Lyon 1-CNRS
Bâtiment Kastler, 10 rue Ada Byron, 69622 Villeurbanne CEDEX, France
E-mail: federico.moretti@mater.unimib.it
E-mail: cristhophe.dujardin@univ-lyon1.fr

[b] Dr. K. Hovvhanesyan, Dr. M. Derdzyan, Prof. A.G. Petrosyan
Institute for Physical Research, National Academy of Sciences
0203 Ashtarak, Armenia

[c] Dr. G. Bizarri, Dr. E. Bourret
Lawrence Berkeley National Laboratory, 1 Cyclotron road, Berkeley, CA 94720, USA

† Now at the Department of Materials Science, University of Milano-Bicocca, Italy
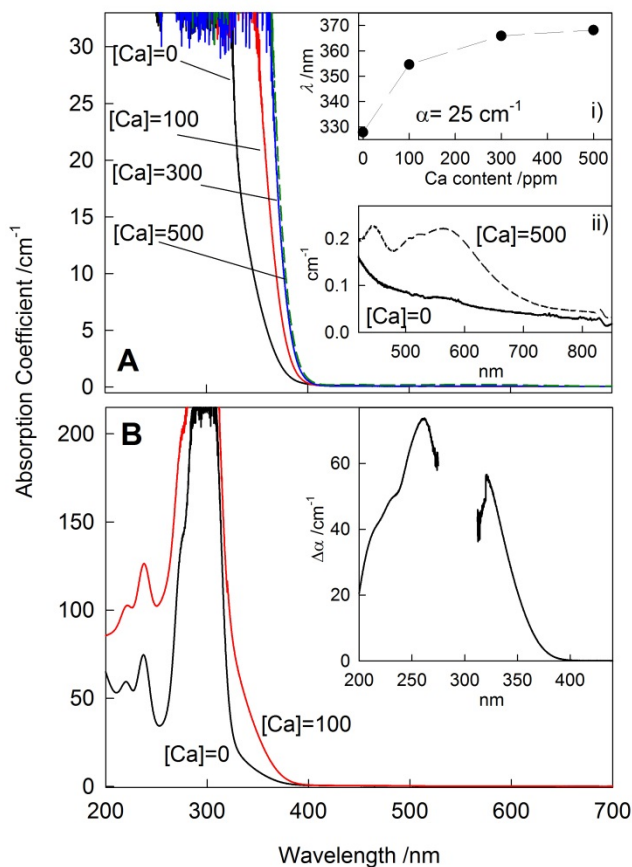
which arise between charge trapping and recombination is

Figure 1. Optical absorption spectra of YAP:Ce,Ca single crystals as a function of calcium concentration for all 2 mm thick samples (panel A) and about 0.25 mm thin ones for [Ca]=0 and 100 ppm (panel B). Insets of panel A: i) wavelength position as a function of Ca content of the absorption threshold evaluated at the absorption coefficient value of 25 cm^{-1}, the line is only a guide for the eyes; ii) enlargement of the 420-850 nm absorption region for [Ca]= 0, and 500 ppm. Panel B inset, absorption coefficient difference between Ca 100 ppm codoped YAP:Ce,Ca and YAP:Ce thin samples; the data related to the 270-310 nm interval have been omitted because of parent measurement saturation.

wavelengths until, for the two highest Ca contents, the position of the absorption tail seems to be practically stable. In the case of 500 ppm Ca codoped sample, other much less intense absorptions appear in the visible region (see inset ii of fig. 1-A) of the spectrum with maxima at about 450 and 590 nm. In order to have a clearer picture on the Ca-related effect, OA measurements were also performed on thin samples (fig. 1-B) (thickness of about 0.25 mm). The spectrum of YAP:Ce clearly shows the presence of several absorption maxima (at about 210, 240, and 300 nm), related to Ce^{3+} 4f-5d transitions, and a relatively weak absorption tail extending up to 370 nm. In the case of the Ca 100 ppm containing sample, this picture is modified by a more pronounced absorption tail and a more intense absorption over the entire 200-290 nm region. The difference among the two spectra, reported in the inset of fig. 1-B, clearly shows the presence of broad band(s) with a maximum at about 260 nm. A further measurement performed on a 200 ppm Ca codoped samples, not reported, confirmed a clear increase of this absorption band with increasing Ca concentration. It has to be noted that the shape of the Ca-induced absorption is not fully accurate: the 280-320 nm region,

in particular, is strongly affected by distortions related to the very high absorption optical density which leads to spectrophotometer saturation, to response nonlinearity, and to sample luminescence issues.

Double substitution of Ca and Ce in nearby located Y^{3+} sites is expected to favour Ce^{4+} states formation for charge compensation, as it has been observed for other Ce-doped materials with divalent codoping (like, for instance, YAG:Ce,Ca,[24] LYSO:Ce,Ca,[16] GAGG:Ce,Ca,[25] LuAG:Ce,Mg,[19] and LuAG:Ce,Ca[26]). Moreover, considering the general trends of the position of Ce^{3+} levels (end state of the charge transfer (CT) transition of Ce^{4+}) in the band gap of oxides,[27] the detected Ca-induced UV absorption is very likely related to the formation of Ce^{4+} ions and to their CT transition. This interpretation is also supported by results obtained on YAP:Ce crystals treated in either oxidizing or reducing atmosphere.[28] Oxygen vacancy formation is expected in the presence of isolated Ca^{2+} ions,[29] possibly causing the weak absorptions in the visible detected exclusively for the largest calcium content.
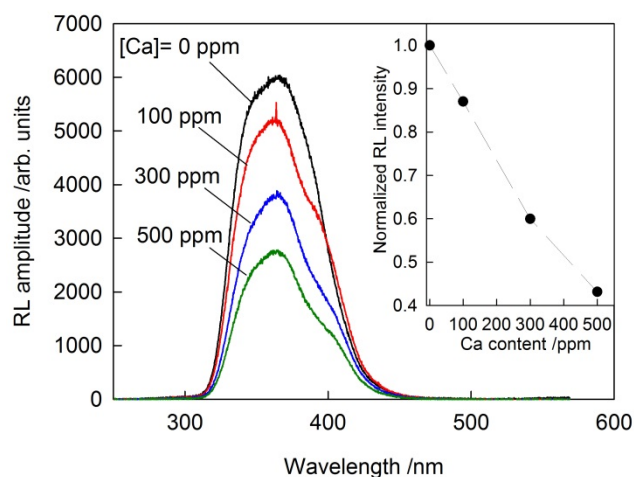

Figure 2. Room temperature RL measurements obtained on YAP:Ce,Ca single crystals for different Ca content. Inset, normalized Ce^{3+} RL intensity as a function of Ca concentration obtained after integration of the measurements in the 300-450 nm region, the line is only a guide for the eyes.

Figure 2 presents radioluminescence (RL) measurements obtained on YAP:Ce,Ca samples for different calcium contents and under the same experimental conditions, thus made accurately comparable. The spectra of all samples are characterized by a bright emission centred at about 350 nm typical of Ce^{3+} 5d-4f radiative recombination in YAP.[22,30] Small variations in shape can be seen as the Ca content is increased. Though they do not seem to follow a clear dependence, they are connected to self-absorption induced by the Ca-related absorption tail. This effect is also connected to a reduction, by a factor 2.5, (inset of fig. 2) in the luminescence intensity. Indeed, the RL intensity decreasing trend could be related to the increasing amount of emitted light which is reabsorbed and not reemitted by Ce^{4+} ions. Considering the rather large overlap between the Ce^{3+} emission band and the Ce^{4+} absorption band,

non-radiative energy transfer among excited trivalent and tetravalent ions is expected.
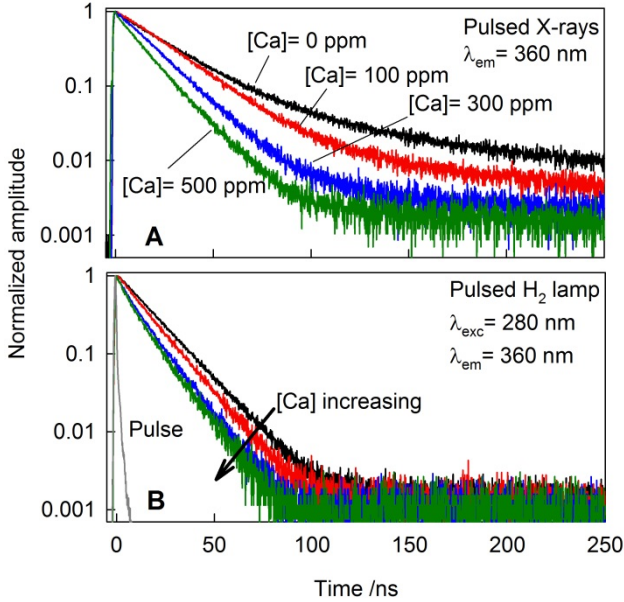

Figure 3. RT pulsed X-ray (A) and optically excited (B) luminescence decays of YAPCe,Ca crystals as a function of Ca codoping. Emission wavelength 360 nm, excitation wavelength for the optically excited decays 280 nm.

Scintillation decay measurements, performed by using pulsed X-ray excitation, were carried out to evaluate the effect of Ca codoping on the timing performances of the samples. The decay curves, reported in fig. 3-A, are clearly modified by the increase in Ca content. In the case of the YAP:Ce sample, the decay is similar to those reported in the literature[31] and is characterized by a fast component, with decay time of about 26 ns, followed by a second one with a decay time of the order of few hundred ns. The results of fits using a sum of exponential decay components are reported in table 1 for all samples. As the Ca content is increased, the percentage of slow component is reduced gradually by about one order of magnitude. The fast component is affected as well as it becomes faster with increasing Ca content (from 26 to 14 ns).

Table 1. Pulsed photo- and radio-luminesce Ce^{3+} decay times of YAP:Ce,Ca crystals as a function of Ca content obtained by fit of the experimental data using a sum of exponential decay components. Emission wavelength 360 nm, excitation wavelength (for PL results) 280 nm. Errors can be evaluated in 5-10%. The weight of each decay component has been evaluated by using the following formula: $W_j = 100 * A_j\tau_j / \sum_j A_j\tau_j$ where A_j and τ_j are the amplitude and decay time of the jth component, respectively.

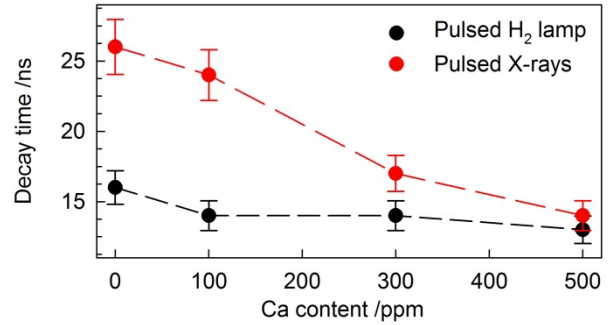| [Ca] ppm	PL		RL	
	τ_1 (ns)	τ_2 (ns)/ weight (%)	τ_2 (ns)/ weight (%)	τ_3 (ns)
0	-	16	26/ 82	131
100	-	14	24/ 91	220
300	7	14/ 77	17/ 91	290
500	5	13/ 80	14/ 93	345

Figure 4. Pulsed photo- and radio-luminescence main Ce^{3+} decay time (τ_2, in table 1) of YAP:Ce,Ca crystals as a function of Ca concentration.

Optically excited luminescence decay measurements (fig. 3-B) have been collected in order to clarify the reasons for the accelerated decay time of the Ce^{3+}. In the case of YAP:Ce, the obtained decay is in good agreement with literature data.[32] As the Ca content is increased, the PL decay becomes faster. For the two highest Ca content, the decays of the luminescence exhibit an identical non-single exponential behaviour. Fit results in terms of exponential decays are reported in table 1. Figure 4 presents a comparison between the main decay time and the Ca content acquired with pulsed X-ray and UV excitation. PL decay measurements were also performed by using a different excitation wavelength (namely 240 nm, not reported): the obtained decays were practically indistinguishable from those reported in fig.3-B and table 1, however with a slightly worse signal to noise ratio.

The Ce^{3+} PL decay acceleration detected by increasing the Ca content in YAP crystals may have several origins. However considering the superposition between the Ce^{3+} luminescence band and the Ce^{4+} absorption, the observed acceleration is the signature of non-radiative energy transfer occurring between Ce^{3+} and Ce^{4+} ions. This process is also responsible for part of the RL intensity reduction detected under steady state X-ray excitation reported above.

The clear difference between the Ce^{3+} luminescence decays in YAP crystals obtained by X-ray and UV photons has already been discussed in detail (see e.g. ref. [33]), and it has been related to the presence of defects acting as traps for charge carriers created during X-ray excitation which delays the prompt recombination process of the carrier themselves on Ce ions. As clearly visible from table 1 and figure 4, the main scintillation decay component becomes closer and closer to the one obtained by UV stimulation as the Ca content is increased, thus suggesting a decreasing role of traps in the scintillation decay results. In order to test this

observation, thermally stimulated luminescence measurements (TSL) have been performed by irradiating the samples with X-rays at 78 K; RL sensitization curves have also been collected during irradiation for each sample. The results are reported in figure 5-A and B for the sensitization and the TSL, respectively.

Steady state RL measurements at 78 K monitored on Ce^{3+} luminescence as a function of time (fig. 5-A) are clearly affected by the amount of Ca present in YAP crystals: the RL amplitude increases by about 10% over the 5 minutes of irradiation in the case of YAP:Ce. As the Ca content is increased, this amplitude rise becomes less evident and almost negligible in the case of the 500 ppm Ca codoped sample. Also the very short phosphorescence tail visible at the end of the irradiations appears to be influenced by Ca content with a clear decreasing trend as the codopant concentration is increased.

The TSL glow curve (Fig. 5-B) of YAP:Ce sample is composed of at least four peaks whose positions are in good accordance with literature data.[33-35] The presence of other trapping states outside the investigated temperature interval is also probable. The amplitude of all glow peaks is strongly reduced by increasing the Ca concentration in the samples, and only the 100 K peak remains visible in the case of the 300 and 500 ppm Ca codoped samples. The overall reduction in amplitude of the 100 K peak is about one order of magnitude between YAP:Ce and YAP:Ce, 500 ppm Ca (inset of figure 5-B).

The above results and the scintillation decays are evidence of the active role of Ca codoping in the reduction of delayed recombination processes and that of charge carrier trapping probability on defect sites. At the moment, however, it cannot be stated that the lower occurrence of charge trapping in the scintillation mechanism is solely caused by the presence of the additional efficient recombination pathway involving Ce^{4+} ions leading to luminescence, as it has been suggested for garnets and silicates. In fact, Vedda et al.[35] evidenced the non-trivial nature - particularly for the 100 K glow peak - of the TSL mechanism in rare earth doped YAP crystals, and they suggested the possible existence of defect complexes involving intrinsic defects coupled to rare earths. So, it might be possible that the introduction of Ca ions in the matrix could also help in avoiding the formation of such complexes, and as such possibly reduce the number of defects acting as traps for charge carriers.
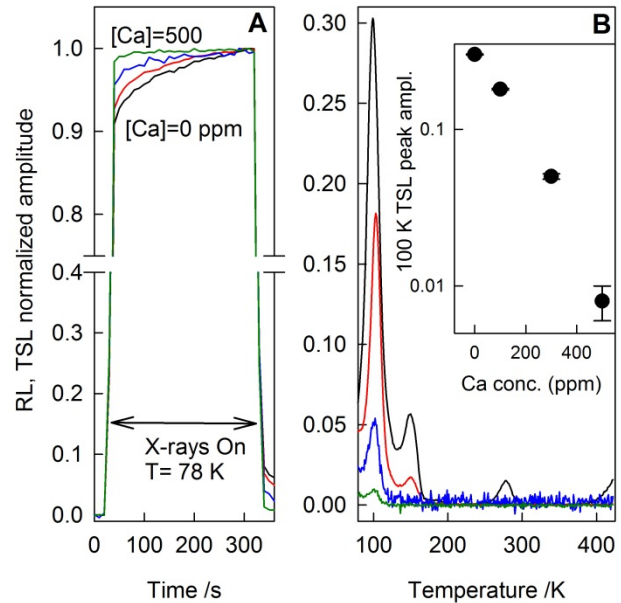

Figure 5. A, Normalized steady state RL measurements performed at 78 K as a function of irradiation time of YAP:Ce,Ca crystals for different calcium concentrations. The normalization has been done on the curve maximum. B, TSL measurements after 78 K irradiations (reported in panel A) obtained with a heating rate of 0.1 K/s. The curves reported in both panels were obtained after integration of the wavelength--resolved results over the Ce^{3+} emission (300-450 nm). Inset of panel B, 100 K TSL peak amplitude as a function of calcium codoping concentration..

Scintillation rise curves for samples with high Ce concentrations (1% Ce) are reported in Fig. 6-A. All the curves are characterized by an increase in the first nanosecond of the RL signal followed by the already discussed scintillation decay. The shape of the rising portion does not show any dependence upon Ca codoping content, with the observed rise being the intrinsic scintillation rise time of these YAP:Ce,Ca samples. The results are very different if we consider a much lower (100 ppm) Ce concentration, figure 6-B. The scintillation rise occurs over a much longer time scale for YAP: 100 ppm Ce sample. By increasing the Ca content in the crystals the scintillation maximum shifts rapidly toward shorter times becoming closer to those detected in the case of the high Ce content samples.

The results of exponential fits to saturation of the rising portion the experimental curves are reported in figure 6-C. These results highlight the remarkably different behaviour of the scintillation rise time between the two sample sets as a function of Ca codoping. The calculated rise time for the samples containing 1 at% cerium is always of the order of 0.3 ns irrespective of the Ca codopant amount while for the low Ce content sample rise times decrease from 3 ns to 0.6 ns as the Ca codoping is increased. The different rise time dependence upon Ca content of the two sample sets is likely related to the average migration distance travelled by charge carriers before their recombination on the luminescence centres. For the 100 ppm Ce doped samples the average distance among cerium ion is of the order of 14 nm and it is reduced to about 3 nm in the case of the 1 at% Ce doping. The results displayed in fig. 6 also show that hole migration and capture are the limiting processes responsible for the quite long scintillation rise time detected for YAP: 100 ppm Ce. Indeed, Ce^{4+} ions are

involved in a recombination process which does not require hole capture as the first necessary step in order to give rise to luminescence, substantially bypassing hole migration and capture. As the Ce^{4+} ion concentration is increased by increasing the amount of Ca in the matrix, hole migration and capture processes become less important leading to faster scintillation rise times.
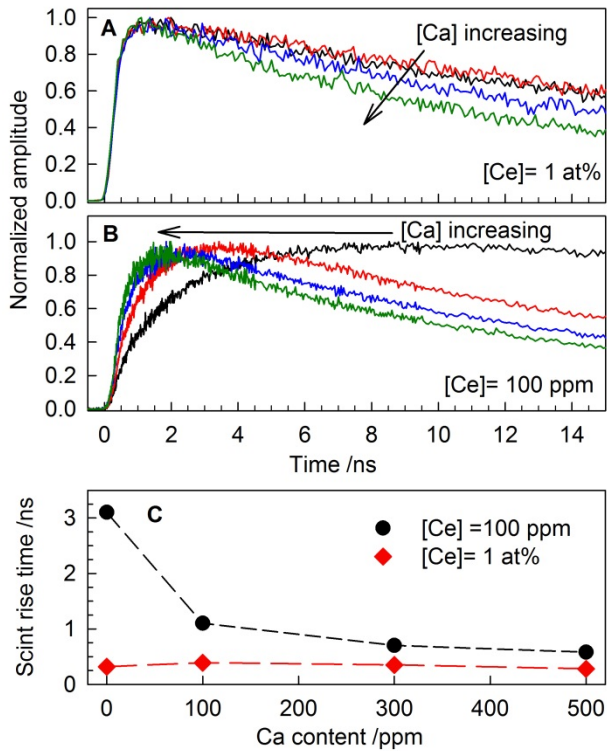
Scheme 1. Room temperature pulsed X-ray luminescence rise (and decay) time measurements obtained on YAP: 1 at.% Ce,Ce (A) and YAP: 100 ppm Ce,Ca (B) single crystals for different Ca codoping concentrations in the 0-500 ppm interval. Panel C reports the rise time as a function of the Ca content obtained after a fit of the experimental curves in terms of an exponential rise to saturation followed by exponential decays. The lines are only a guide for the eyes.

Scintillation pulse height spectrum (that provides light yield) is a useful tool to characterize the overall efficiency of samples under mono-energetic γ-ray source. The results (reported in figure 7 for all the samples doped with 1 at% Ce) show the reduction in scintillation efficiency as the Ca content is increased, with the photopeak quickly disappearing and a shift of the Compton edge position toward lower values. This reduction of scintillation efficiency is likely related, as already mentioned following results from other kind of measurements, to reabsorption of the emitted light by Ce^{4+} ions as well as energy transfer phenomena between Ce^{3+} and Ce^{4+} ions.
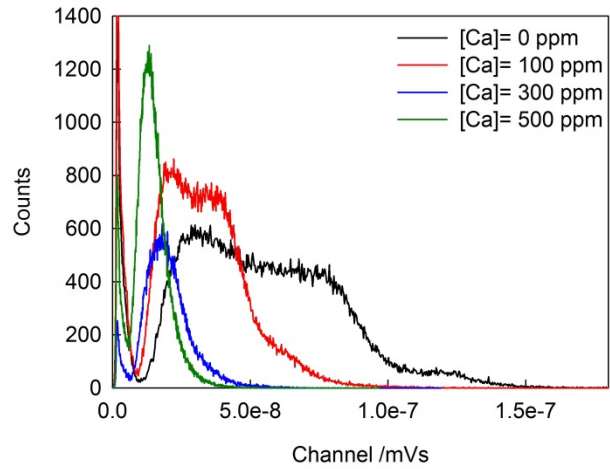

Figure 1. Pulse height spectra obtained on YAP:Ce,Ca crystal for different Ca contents by using a ^{137}Cs radioactive source.

From the results above, Ca codoping does not appear as an appropriate strategy to improve the scintillation characteristics of YAP:Ce crystals, in contrast to what is observed for Ce-doped orthosilicates and garnets. Ca codoping is acting similarly in all matrices – favouring the oxidation of Ce^{3+} ions into tetravalent ones with a substantial reduction in the effects related to electron trapping on defect sites (delayed recombination, afterglow, and hysteresis)– but in YAP these improvements are outweighed by reabsorption and energy transfer phenomena involving the two cerium ion valencies. These unwanted phenomena are only related to the closer energy separation between the Ce^{4+} CT absorption and the Ce^{3+} 5d-4f radiative recombination in YAP. For the very same reason, this codoping strategy is not expected to work for Pr^{3+} doped oxides, since the Pr^{4+} CT absorption is expected to be at even lower energies than those of Ce^{4+},[27] thus partially, if not completely, superimposed to the Pr^{3+} 5d-4f radiative recombination; indeed, this has been recently reported[36] for LuAG:Pr,Mg. A similar strategy, but using different codopants, should be effective for Eu^{2+} doped materials, since the Eu^{3+} CT transition is usually located in the deep UV and the Eu^{2+}-related emission in the violet-green region of the electromagnetic spectrum.

On a more general note, this charge carrier recombination sequence manipulation strategy could have a much wider applicability for both other oxidic matrices, such as Ce doped lutetium pyrosilicate – $Lu_2Si_2O_7$:Ce, and on non-oxidic ones, such as halides. The latter case appears particularly enticing considering that CsI:Tl (a rather inexpensive and very bright scintillator commonly used, for instance, in radiography and radioscopy) is known to have defect related phenomena which limit its use, and several strategies have been proposed to limit the role of defects. In particular, codoping with aliovalent[37-39] ions (Eu, Sm, Bi) has been already proposed, but the mechanism leading to scintillation improvements has not been fully elucidated. The Tl activator differs from Eu and Ce by its valence (Tl^+ in CsI vs Eu^{3+} and Ce3+ in the concerned oxides). We wonder whether the already proposed codoping in CsI:Tl could actually behave similarly to that mentioned for oxide matrices by favouring a partial change in Tl valence state in the crystals. We also wonder

whether this kind of strategy could work by using an anionic substitution instead of a cationic one. This would be an additional tool to tailor the scintillation timing performance, as well as reducing the role of stable traps and would be an alternative to a recently proposed strategy that is to introduce voluntarily deep traps.[15]

Conclusions

The effects of Ca-codoping on YAP:Ce single crystal optical and scintillation properties have been studied. It was found that Ca codoping lowers the charge carrier trapping probability on defect sites and reduces the probability of delayed recombination processes in scintillation. We also demonstrate that hole trapping is the limiting factor for rise time response of cerium doped scintillators when sequential trapping is involved. This co-doping strategy aiming at the conversion of Ce^{3+} into Ce^{4+}, combined with an appropriate activator concentration, enables controlling the rise time which is crucial for fast timing applications such as time-of-flight detection technique. However, contrary to observations in garnets and silicates scintillating crystals where Ca (and Mg) codoping proved to be a useful way to improve the scintillation characteristics (light yield and timing performances) of such matrices, in the case of YAP:Ce crystals, the light yield is decreased. Ca induced partial oxidation of Ce^{3+} ions leads to non-radiative energy transfer between Ce^{3+} and Ce^{4+}, reducing the luminescence efficiency. This strategy cannot, then, be considered particularly useful for YAP:Ce. However, the presented data points to codoping strategies for other activator ions and different matrices. Moreover, they also provide further insights in understanding of charge carrier migration and trapping phenomena occurring in the scintillation process.

Experimental Section

Single crystal of orthorhombic $YAlO_3$:Ce,Ca (YAP:Ce,Ca) were grown by the Czochralski method in pure Ar atmosphere using a 40 mm diameter Ir crucible. High purity Y_2O_3, CeO_2, $CaCO_3$ powders and crystalline Al_2O_3 were used as starting materials. An undoped YAP single crystal rod oriented along the <b> axis was used as a seed. The Ce concentration in the melt was set for all the samples equal to 1 at%. The concentration of added Ca was varied from 0 to 500 ppm (100, 300, and 500 ppm). Single crystals of about 15 mm in diameter and 20-25 mm long were pulled at a 2 mm/h and 30 rpm rotation rate. An additional set of samples characterized by a Ce content of 100 ppm (same amount of Ca: 100, 300 and 500 ppm) has also been included only for scintillation rise time measurements. Considering the ionic radii of Ce^{3+} and Ca^{2+} (1.143 Å and 1.12 Å, respectively), both Ce and Ca are expected to occupy Y^{3+} (radius 1.019 Å) lattice sites with a 8-fold oxygen coordination, but swollen by a next oxygen and aluminium cations.[40] The effective distribution coefficient of Ce in YAP is 0.45.[41]

Optically polished 7x7x2 mm^3 plates were obtained from all crystal compositions. Additionally, 0.25 mm thick samples were prepared from YAP:Ce singly doped and 100 ppm Ca codoped specifically for optical absorption. All of the samples were cut from approximately the same crystal areas at a distance of 12-17 mm from the top of the boules. Sample examination with a MPS-2 polarizing microscope revealed no second phase precipitations, light scattering inclusions or twins. Optical absorption measurements were collected in the 200-800 nm range with a SPECORD 200 PLUS spectrometer.

Room temperature radioluminescence (RL) measurements were obtained by using a Philips X-ray tube operated at 30 kV, collecting the emitted light with an optical fibre and detected by an Andor Newton EMCCD coupled to an Andor Shamrock 500i monochromator. The obtained spectra were not corrected for the experimental response of the detection system. Spectrally resolved thermally stimulated luminescence measurements were performed in the 78-423 K interval with a heating rate of 0.1 K/s by using the same light detection chain and irradiation source (set at 30 kV with an irradiation time of 300 s) used for RL measurements, and by employing a Linkam HFS600 liquid nitrogen-cooled stage.

Time resolved photoluminescence results have been obtained with a time correlated single photon counting (TCSPC) system composed by an IBH H_2 pulsed lamp (pulse full width at half maximum 1 ns), a fast photomultiplier (SMA650) and TCSPC electronics (PicoHarp 300) both from PicoQuant. Excitation and emission wavelength selection was done by the use of interferential filters (Andover corp.) with a bandpass of 10 nm. Pulsed X-ray decay measurements were performed with the same light collection system and a Hamamatsu N5084 light-excited X-ray tube set at 30 kV as irradiation source. The optical excitation of the tube was performed with a Hamamatsu PLP-10 picosecond light pulser. In both cases, decay curve fits were done without considering the convolution between the pulse and the exponential decay component(s).

Pulsed X-ray scintillation rise (and decay) measurements have been performed at LBNL with the instrumentation reported in reference [42]. The instrument response function (IRF) full width at half maximum is about 100 ps. The scintillation rise fits have been performed considering an exponential growth to saturation followed by exponential decay components without considering the convolution with the IRF. The obtained rise time values are, then, only qualitative in nature.

Pulse height spectra of all the studied samples were collected by using a Photonis XP2020Q photomultiplier, data were acquired by a Lecroy LT372 digital oscilloscope and processed by a homemade software. The excitation source was a ^{137}Cs source emitting γ-rays with an energy of 661.7 keV. Each sample was coupled to the PMT window using optical grease and was covered with several layers of PTFE film in order to collect most of the emitted light.

Acknowledgements

[1]   C. Ronda, H. Wieczorek, V. Khanin, P. Rodnyi *ECS J. Sol. State Sci. And Tech.* **2016**, *5*, R3121-R3125
[2]   C. L. Melcher *J. Nucl. Med.* **2000**, *41*, 1051-1055
[3]   M. Korjik, E. Auffray *IEEE Trans. Nucl. Sci.* **2016**, *63*, 552-563
[4]   P. Lecoq, A. Annekov, A. Gektin, M. Korzhik, C. Pedrini *Inorganic Scintillators for Detector Systems*, Springer-Verlag, Berlin, 2006
[5]   M. Nikl, A. Yoshikawa *Adv. Optical. Mater.* **2015**, *3*, 463-481
[6]   R. Kirkin, V. V. Mikhailin, A. N. Vasil'ev, *IEEE Trans. Nucl. Sci.* **2012**, *59*, 2057-2064
[7]   A. Belsky, K. Ivanovskikh, A. Vasil'ev, M. F. Jubert, C. Dujardin, *J. Phys. Chem Lett.* **2013**, *4*, 3534-3538
[8]   S. Gridin, A. Belsky, C. Dujardin, A. Gektin, N. Shiran, A. Vasil'ev, *J. Phys. Chem. C* **2015**, *119*, 20578-20590

[9]   E. Dell'Orto, M. Fasoli, G. Ren, A. Vedda, *J. Phys. Chem. C* **2013**, *117*, 20201-20208.

[10]   F. Moretti, G. Patton, A. Belsky, M. Fasoli, A. Vedda, M. Trevisani, M. Bettinelli, C. Dujardin, *J. Phys. Chem. C* **2014**, *118,* 9670-9676.

[11]   K. Kamada, T. Endo, K. Tsutumi, J. Pejchal, M. Nikl, *Cryst. Growth Des.* **2011**, *11*, 4484-4490

[12]   M. Fasoli, A. Vedda, M. Nikl, C. Jiang, B. P. Uberuaga, D.A. Anderson, K. J. McClellan, C. R. Stanek, *Phys. Rev. B: Condens. Matter Mater. Phys.* **2011**, *84,* 081102

[13]   M. Nikl, *Phys. Status Solidi A* **2000**, *178*, 595-620

[14]   A. Gektin, A. Belsky, A. Vasil'ev, *IEEE Trans. Nucl. Sci.* **2014,** *61,* 262-

[15]   F. Moretti, G. Patton, A. Belsky, A. G. Petrosyan, C. Dujardin, *Phys. Chem. Chem. Phys.* **2016**, *18*, 1178-1184

[16]   S. Blahuta, A. Bessière, B. Viana, P. Dorenbos, V. Ouspenski, *IEEE Trans. Nucl. Sci.* **2013**, *60*, 3134-3141

[17]   S. R. Kärner, V. V. Laguta, M. Nikl, T. Shalapska, S. Zazubovich, *J. Appl. Phys. D: Appl. Phys.* **2014**, *47*, 065303

[18]   S. Liu, X. Feng, Z. Zhou, M. Nikl, Y. Shi, Y. Pan, *Phys. Status. Solidi (RRL)* **2014**, *71,* 105

[19]   M. Nikl, K. Kamada, V. Babin, J. Pejchal, K. Pilarova, E. Mihokova, A. Bleiterova, K. Bartosiewicz, S. Kurosawa, A. Yoshikawa, *Cryst. Growth Des.* **2014,** *14,* 4827

[20]   M. Nikl, V. Babin, J. A. Mares, K. Kamada, S. Kurosawa, J. Tous, J. Houzvicka, K. Blazek, *J. Lumin.* **2016,** *169,* 539-543.

[21]   F. Moretti, A. Vedda, N. Chiodini, M. Fasoli, A. Lauria, V. Jary, R. Kucerkova, E. Mihokova, A. Nale, M. Nikl, *J Lumin.* **2012**, *132*, 461-466.

[22]   M. J. Weber, *J. Appl. Phys.* **1973**, *44,* 3205

[23]   M. Alshourbagy, S. Bigotta, D. Herbert, A. Del Guerra, A. Toncelli, M Tonelli, *J. Cryst. Growth* **2007**, *303*, 500-505

[24]   S.R. Rotman, H.L. Tulle, C. Wardeb, *J. Appl. Phys.* **71**, 1992, 1209-1214

[25]   Y. Wu, F. Meng, Q. Li, M. Koschan, C. Melcher, *Phys. Rev. Appl.* **2014**, *2*, 044009/1-13

[26]   A.G. Petrosyan, K.L. Ovanesyan, M.V. Derdzyan, I. Ghambaryan, G. Patton, F. Moretti, E. Auffray, P. Lecoq, M. Lucchini, K. Pauwels, C. Dujardin, *J. Cryst. Growth* **2015**, *430*, 46-51

[27]   P. Dorenbos, *J. Phys.: Condens. Matter* **2003**, *15,* 8417-8433

[28]   D. Cao, G. Zhao, J. Chen, Q. Dong, Y. Ding, Y. Cheng, *J Alloys Compd.* **2010**, *489*, 515-518.

[29]   M. M. Kuklja, *J. Phys.: Condens. Matter* **2000**, *12*, 2953-2967

[30]   A. Lempicki, M. R. Randles. D. Wissiewski, M. Balcerzyk, C. Brecher, A. J. Wojtowicz, *IEEE Trans. Nucl. Sci.* **1995**, *42*, 280-284

[31]   M. Moszynski, M. Kapusta, D. Wolski, W. Klamra, B. Cederwall, *Nucl. Instrum. Methods Phys. Res. A* **1998**, *404,* 157-165

[32]   J. A. Mares, M. Nikl, C. Pedrini, B. Moine, K. Blazek, *Material Chem. Phys,* **1992**, *32,* 342-348

[33]   A. J. Wojtowicz, J. Glodo, W. Drozdowski, K. R. Przegietka, *J. Lumin.* **1998**, *79,* 275-291

[34]   M. Zhuravleva, A. Novoselov, E. Mihokova, J. A. Mares, A. Vedda, M. Nikl, A. Yoshikawa, *IEEE Trans. Nucl Sci.* **2008**, *55,* 1476-1479

[35]   A. Vedda, M. Fasoli, M. Nikl, V. V. Laguta, E. Mihokova, J. Pejchal, A. Yoshikawa, M. Zhuravleva, *Phys. Rev. B: Condens. Matter Mater. Phys.* **2009**, *80*, 045113

[36]   J. Pejchal, M. Buryi, V. Babin, P. Pruza, A. Bleiterova, J. Barta, L. Havlak, K. Kamada, A. Yoshikawa, V. Laguta, M. Nikl, *J. Lumin.* **2017**, *181*, 277-285.

[37]   V. V. Nagarkar, S. C Thaker, V. Gaysinskiy, L. E. Ovechkina, S. R. Miller , S. Cool, C. Brecher, *IEEE Trans. Nuclear Sci.* **2009**, *56*, 565

[38]   E. E. Ovechkina, V Gaysinskiy, S. R. Miller, C. Brecher, A. Lempicky, V. V. Nagarkar, *Rad. Measurements* **2007**, *42*, 541-544

[39]   D. Totsuka, T. Yanagida, Y. Fujimoto, Y. Yokota, F. Moretti, A. Vedda, A. Yoshikawa, *Appl. Phys. Express* **2012**, *5*, 052601

[40]   E. Gallucci, C.Dujardin, M. Boudeulle, C. Pedrini, A.G. Petrosyan, T. Hansen in *Proceedings of the fifth International Conference on Inorganic Scintillators and Their Application, SCINT'99,* (Ed. V. Mikhailin), Moscow State University, 1999, pp. 506-510

[41]   B. Perner, J. Kvapil, K. Blazek, J. Horak, J. Kvapil, B. Manek, *Acta Physica Hungarica* **1987**, *61*, 231-234

[42]   S. E Derenzo, M. J. Weber, W. W. Moses, C. Dujardin, *IEEE Trans. Nucl. Sci.* **2000**, *47,* 860-864

Entry for the Table of Contents (Please choose one layout)

Layout 1:

ARTICLE

Taking a shortcut. Ca codoping in YAlO$_3$:Ce single crystal is able to shorten the scintillation decay time (see figure), though this is also accompanied by a general reduction of the scintillation efficiency. The lower efficiency is mostly related to reabsorption and energy transfer phenomena involving Ce^{3+} and Ce^{4+} ions.
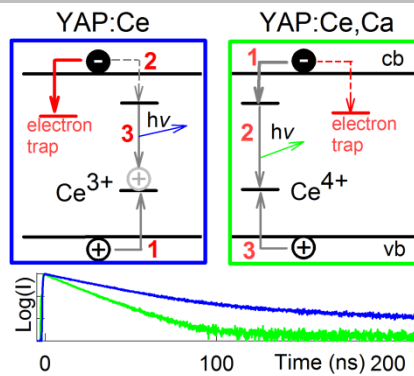
Federico Moretti*, Karine Hovhannesyan, Marina Derdzyan, Gregory A. Bizarri, Edith D. Bourret, Ashot Petrosyan, and Christophe Dujardin*

Page No. – Page No.

Consequences of Ca codoping in YAlO$_3$:Ce single crystals